The $P2Y_2$ Receptor Agonist INS37217 Stimulates RPE Fluid Transport In Vitro and Retinal Reattachment in Rat

Arvydas Maminishkis,[1] *Stephen Jalickee,*[1] *Sasha A. Blaug,*[2] *Jodi Rymer,*[2] *Benjamin R. Yerxa,*[3] *Ward M. Peterson,*[3] *and Sheldon S. Miller*[1,2]

Purpose. To investigate the effects of INS37217, a synthetic $P2Y_2$ receptor agonist, on intracellular calcium signaling, electrophysiology, and fluid transport in vitro and on experimentally induced retinal detachment in rat eyes in vivo.

Methods. Freshly isolated monolayers of bovine and human fetal RPE were mounted in Ussing chambers for measurements of cytosolic calcium levels ($[Ca^{2+}]_i$), membrane voltages and resistances, and transepithelial fluid transport. Retinal detachments were experimentally produced in Long-Evans rats by injecting modified phosphate-buffered saline into the subretinal space (SRS). Experimental or vehicle solutions were injected into the vitreous, and the size of blebs in the SRS was scored under masked conditions.

Results. Addition of INS37217 to Ringer's solution bathing the apical membrane transiently increased $[Ca^{2+}]_i$, altered membrane voltages and resistances and generally produced responses that were similar in magnitude to those of uridine triphosphate (UTP). In fluid transport experiments performed with the capacitance probe technique, INS37217 significantly increased fluid absorption across freshly isolated bovine and fetal human RPE monolayers. All in vitro results were blocked by apical 4,4′-diisothiocyanatostilbene-2,2′-disulfonic acid (DIDS), which has been shown to block $P2Y_2$ receptors in the RPE. Intravitreal administration of INS37217, but not UTP, in the rat model of retinal detachment enhanced the removal of SRS fluid and facilitated retinal reattachment when compared with vehicle control.

Conclusions. These findings indicate that INS37217 stimulates the RPE fluid "pump" function in vitro by activating $P2Y_2$ receptors at the apical membrane. In vivo INS37217 enhances the rates of subretinal fluid reabsorption in experimentally induced retinal detachments in rats and may be therapeutically useful for treating a variety of retinal diseases that result in fluid accumulation in the subretinal space. (*Invest Ophthalmol Vis Sci.* 2002;43:3555–3566)

P2Y receptors are activated by extracellular nucleotides and belong to the superfamily of metabotropic G-protein–coupled receptors.[1] The $P2Y_2$ receptor subtype has approximately equal affinity for extracellular ATP and UTP. Activation of $P2Y_2$ receptors has been shown to stimulate release of cytosolic Ca^{2+} from intracellular stores through G_q-mediated activation of phospholipase C (PLC)-β and the subsequent generation of inositol trisphosphate (IP3).[2] In a wide variety of epithelial tissues throughout the body, $P2Y_2$ receptor activation is associated with a number of physiological functions, including ion and fluid transport, mucin and glycoprotein release, cell volume regulation, surfactant release, and regulation of cilia beat.[3] Previous in vitro and in vivo studies in the eye have demonstrated pharmacologic and biochemical evidence for $P2Y_2$ receptors in the retinal pigment epithelium (RPE), ciliary epithelia, lens epithelium, corneal epithelium, and conjunctiva.[4–11]

The RPE passively and actively transports fluid in the subretinal-to-choroidal direction, and this RPE fluid "pump" function is thought to play a major role in reabsorption of subretinal fluid and in promoting and maintaining retinal attachment.[12] The polarized distribution of ion channel and transporter proteins at apical and basolateral membranes allows the RPE to carry out net vectorial transport of ion and fluid between the subretinal space (SRS) and the blood.[13] These proteins can be regulated by activation of surface receptors on apical and basolateral membranes through the action of a variety of paracrine, autocrine, and hormonal signaling molecules, which can influence both the directionality and magnitude of fluid transport across the RPE.[14–20] For example, in freshly isolated monolayers of bovine RPE, activation of $P2Y_2$ receptors by addition of uridine triphosphate (UTP) to Ringer's solution bathing the apical membrane has been shown to stimulate fluid absorption transiently by approximately 150% above prestimulation levels.[20] Stimulation of RPE fluid absorption in vivo is expected to enhance the net transport of fluid in the subretinal-to-choroidal direction. A major objective of the present study was to investigate the effects of natural and synthetic $P2Y_2$ receptor agonists (UTP and INS37217, respectively) in vivo in stimulating reabsorption of subretinal fluid in an experimental model of retinal detachment. INS37217 is a synthetic $P2Y_2$ receptor agonist engineered with enhanced metabolic stability and resistance to extracellular nucleotidase-mediated hydrolysis.[21,22] In the present study, the effects of INS37217 on a variety of RPE cellular functions were investigated, including mobilization of cytosolic Ca^{2+} levels, ion transport in vitro, and fluid transport in vitro and in vivo. Our collective findings demonstrate that INS37217 stimulates intracellular Ca^{2+} $[Ca^{2+}]_i$-signaling and ion-coupled fluid transport in vitro and that intravitreally administered INS37217, but not UTP, stimulates subretinal fluid reabsorption in a rat model of retinal detachment.

Methods

In Vitro Preparation

Bovine eyes were obtained from a nearby abattoir (Rancho Veal, Petaluma, CA), placed in cold HCO_3 Ringer's solution 15 to 30 minutes

From the [1]School of Optometry and [2]Department of Molecular and Cell Biology, University of California, Berkeley, Berkeley, California; and [3]Inspire Pharmaceuticals, Durham, North Carolina.

Supported by National Eye Institute Grant EY02205 (SSM) and Core Grant EY03176, and Inspire Pharmaceuticals.

Submitted for publication December 20, 2001; revised April 29, 2002; accepted June 18, 2002.

Commercial relationships policy: I, E (BRY, WMP); P (BRY); F, C (SSM); N (AM, SJ, SAB, JR).

The publication costs of this article were defrayed in part by page charge payment. This article must therefore be marked "*advertisement*" in accordance with 18 U.S.C. §1734 solely to indicate this fact.

Corresponding author: Sheldon S. Miller, NIH/NEI, Building 31, Room 6A03, 31 Center Drive MSC 2510, Bethesda, MD 20892-2510; millers@nei.nih.gov.

after death, and transported to the laboratory. The eyes were kept in cold Ringer's solution, bubbled with 8% CO_2, 10% O_2, balance N_2 and remained viable for up to 8 hours after enucleation. The anterior portion of the eye was removed before sectioning the posterior portion into quarters. The vitreous was carefully removed and the retina peeled away. A circular area of RPE-choroid was cut out, peeled away from the sclera, placed on a supporting mesh, and mounted apical side up between the two halves of a modified Ussing chamber. Perfusion of Ringer's solution into the apical and basal baths was controlled separately.[23]

Solutions

Control Ringer's solution contained the following (in mM): 120 NaCl, 5 KCl, 23 $NaHCO_3$, 1 $MgCl_2$, 1.8 $CaCl_2$, 2.0 taurine, and 10 glucose. This solution was bubbled continuously with 8% CO_2, 10% O_2, balance N_2 (pH ~7.4) and osmolarity of the Ringer's solution was 295 ± 5 mOsM. Glutathione (1 mM) was added to solutions minutes before perfusion. UTP, 4,4′-diisothiocyanatostilbene-2,2′-disulfonic acid disodium salt (DIDS), and 1,2-bis (2-aminophenoxy)ethane-*N*,*N*,*N*′*N*′-tetra acetic acid (BAPTA) were obtained from Sigma Chemical Co. (St. Louis, MO). All solutions were made iso-osmotic. Fura-2 was obtained from Molecular Probes (Eugene, OR). INS37217 was obtained from Inspire Pharmaceuticals (Durham, NC).

Electrophysiology

Calomel electrodes in series with Ringer's solutions and agar bridges were used to measure the transepithelial potential (TEP), and the intracellular microelectrode signals were referenced to either the apical or basal bath to measure the membrane potentials, V_A and V_B, where TEP = $V_B - V_A$. Conventional microelectrodes were made from borosilicate glass tubing of 0.5 mm inner diameter and 1 mm outer diameter with a filament (Sutter Instrument Co., Novato, CA), were back filled with 150 mM KCl, and had resistances of 80 to 200 MΩ.

The total transepithelial resistance (R_T), and the ratio of the apical to basolateral membrane resistance (R_A/R_B) were obtained by passing 4 μA current pulses (8 μA peak to peak) across the tissue and measuring the resultant changes in TEP, V_A, and V_B. Current pulses were bipolar, with a period of 3 seconds. R_T is the resultant change in TEP divided by 4 μA, and R_A/R_B is the absolute value of the change in V_A divided by the change in V_B ($R_A/R_B = \Delta V_A/\Delta V_B$). The current-induced voltage deflections were digitally subtracted from the records for clarity. The control Ringer's solution for measurements of TEP and R_T contained (in mM): 120 NaCl, 5 KCl, 23 $NaHCO_3$, 1 $MgCl_2$, 1.8 $CaCl_2$, and 5 glucose. In the electrophysiology experiments (see Figs. 3, 4), the black bar indicates a solution change at the manifold outside of the recording chamber. In some cases the response onset was variably delayed because of "dead space" in the fluid delivery system and because of thickness variations in the unstirred layer at the apical membrane.

Equivalent Circuit

The RPE electrical properties can be modeled by the equivalent circuit shown in Fig. 1. The apical and basolateral membranes of the RPE are each represented as an equivalent electromotive force (EMF), E_A or E_B, in series with a resistor, R_A or R_B, respectively. The paracellular pathway is represented as a shunt resistor (R_S), which is the parallel combination of the junctional complex resistances between neighboring cells and the resistance caused by the less-than-perfect mechanical seal around the circumference of the tissue. Because of this shunt resistance and the differences between the membrane EMFs, a current (I_S) flows around the circuit. The observed membrane potentials V_A and V_B are given by

$$V_A = E_A - I_S \cdot R_A \quad (1)$$

$$V_B = E_B + I_S \cdot R_B \quad (2)$$

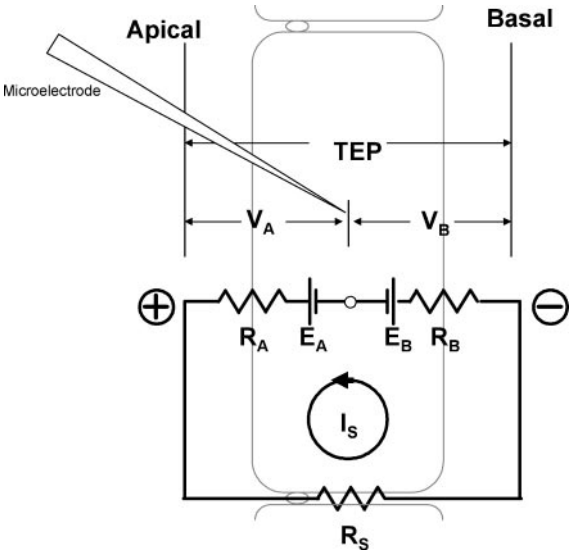

FIGURE 1. RPE equivalent circuit superimposed on a schematic RPE cell. R_A and R_B represent the resistances of the apical and basolateral membranes. R_S represents the shunt resistance, a parallel combination of the junctional complex resistance and the resistance of the mechanical seal at the circumference of the tissue. The apical and basolateral membrane EMFs are represented by E_A and E_B. Because of the differences between E_A and E_B, a current loop (I_s) flows through the circuit. A microelectrode placed in the cell is used to measure the measured apical and basolateral membrane potentials, V_A and V_B, relative to reference electrodes in the apical and basal baths, respectively. The transepithelial potential or TEP = $V_B - V_A$.

The effect of this loop current is to depolarize the apical membrane and hyperpolarize the basolateral membrane.[23,24] The apical and basolateral membrane voltages are electrically coupled through R_S, so that any voltage change at one membrane is partially shunted to the opposite membrane (see Fig. 3). For example, if a solution composition change primarily alters E_B, without altering, R_A, R_B, or R_S, then the apical membrane voltage also changes. Most of the resultant change in V_A is a passive consequence of the current shunted from the basolateral membrane.[13,25]

$$\Delta V_A = (R_A/[R_A + R_S]) \cdot \Delta V_B \quad (3)$$

Equation 3 represents a simplified case to illustrate the fractional amount of basolateral membrane voltage change that can appear at the apical membrane. For example, if R_S were close to zero, then this fraction would be close to 1 and $\Delta V_A \approx \Delta V_B$. In contrast, if $R_S >> R_A$ then $\Delta V_A \approx 0$. The transepithelial (or total) resistance R_T is expressed in terms of the membrane and shunt resistances as follows

$$R_T = [(R_A + R_B)R_S]/[R_A + R_B + R_S] \quad (4)$$

If, for example, the basolateral membrane conductance increases (R_B decrease), then R_T should decrease, as predicted by equation 4, and R_A/R_B should increase.

Fluorescence Imaging: $[Ca^{2+}]_i$

Cytosolic free Ca^{2+} levels, $[Ca^{2+}]_i$, were monitored with the fluorometric ratioing dye fura-2 AM (Molecular Probes) in a modified Ussing chamber. The chamber and setup have been described previously.[20,26] In brief, Ringer's solution containing 5 to 10 μM fura-2 AM dissolved in dimethyl sulfoxide (DMSO; containing 10% pluronic acid) was perfused for 30 to 40 minutes over the apical membrane to load the cells. In addition, 1 mM probenecid was included in all loading and subsequent Ringer's solutions to inhibit dye extrusion by the organic anion

transporter located in the apical membrane.[27] Photic excitation was achieved with a xenon light source filtered at 350 and 385 nm (bandwidth, ±10 nm) every 0.5 second, and the fluorescence emission was collected from approximately 10 cells at 510 nm with a photomultiplier tube (Thorn EMI, Salisbury, South Australia, Australia). The ratio of the fluorescence intensities at 350 to 385 nm (R) was determined every second. The technique and computer software for data acquisition have been described previously.[14]

Calibration of $[Ca^{2+}]_i$ was performed at the end of each experiment by first perfusing both membranes with a zero-calcium Ringer's solution containing 10 mM EDTA, which chelates any residual-free calcium, and 10 μM ionomycin, which is a calcium ionophore that facilitates the equilibration $[Ca^{2+}]_i$ and extracellular Ca^{2+} $[Ca^{2+}]_o$. After this zero calcium calibration, the tissue was then exposed to saturating (1.8 mM) concentration of calcium. Then $[Ca^{2+}]_i$ was determined according to the equation $[Ca^{2+}]_i = K(R - R_{min})/(R_{max} - R)$, where R_{max} is the maximum ratio of the fluorescence intensities at 350 and 385 nm, which was determined at the saturating Ca^{2+} signal; R_{min} is the ratio of fluorescence intensities in the absence of $[Ca^{2+}]_o$; K is equal to K_d (F_{min}/F_{max}), where K_d is the dissociation constant for fura-2 AM (220 nM)[28]; and F_{min} and F_{max} are the fluorescence intensities at 385 nm in the absence and presence of saturating $[Ca^{2+}]_o$, respectively.

Fluid Transport

A modified capacitive probe technique, previously described,[15] was used to determine the rate of fluid movement across the RPE. In brief, the RPE was mounted in a water-jacketed Ussing chamber and oriented vertically, with the apical and basolateral membranes separately exposed to Ringer's solution held in the bathing reservoirs. Stainless steel probes (Accumeasure System 1000; MT Instruments, Latham, NY) were lowered into the apical and basolateral bathing wells to measure the capacitance of the air gap between the probe and fluid meniscus. The fluid transport rate, J_V (in microliters per square centimeter per hour), was determined by monitoring the fluid movement–induced changes in the air gap capacitance at the apical and basolateral baths. The probes on both sides of the tissue were backed off from the surface of the Ringer's solution during a bathing solution change. To check that the solution changes per se did not appreciably alter J_V, a control-to-control Ringer's solution change was performed near the beginning of each experiment and at appropriate intervals during the experiment. The capacitance probes were moved away from the bathing reservoirs, and fresh control Ringer's solution was perfused into the chamber. The fluid transport apparatus also allows the experimenter to continuously monitor TEP and R_T, but for technical reasons (solution perfusion rates, TEP, R_T sampling rates, electrode stability) we can only compare the initial changes in TEP and R_T (phase I, see the Results section) with those in the electrophysiology experiments. Experiments were continued only if J_V, TEP, and R_T were not appreciably altered by this control-to-control Ringer's solution change. The water-jacketed Ussing chamber was placed in an incubator to maintain steady state control over temperature (pCO_2) and humidity.

Human Fetal Tissue

The research adhered to the tenets of the Declaration of Helsinki. Research protocols were approved by the University of California Committee for the Protection of Human Subjects. Fetal eyes were obtained by an independent procurer (Advanced Bioscience Resources, Alameda, CA).

In Vivo Preparation: Rat Study Design

All animal experiments were conducted in compliance with the ARVO Statement for the use of Animals in Ophthalmic and Vision Research, and the protocol was approved by the Animal Care and Use Committee of the University of California at Berkeley. Retinal detachments were created in Long-Evans female rats by injecting 2 to 3 μL of modified phosphate-buffered saline (MPBS) Ringer solution into the SRS; only one eye per rat was used. With a charge-coupled device (CCD) camera, images of the subretinal blebs were obtained at 1-minute intervals for several hours. The acquisition of images is described in further detail later. In the control part of each experiment (at 0–30 minutes after creation of the retinal detachment), apparent bleb size reached a steady state size, which remained unchanged during the course of anesthesia (several hours). MPBS solutions, with or without INS37217 (5 mM) were formulated and injected (3 μL) into the vitreous of the rat eye under masked and randomized conditions. The vials and their contents were indistinguishable. After vitreous injection, the apparent bleb size either increased or decreased monotonically or was constant over the next 60 minutes, as judged by the experimenter using the seven rank scale (0 ± 3) illustrated in Figure 9A. Ranks were assigned by observing the change in apparent bleb size between 30 and 90 minutes after drug or placebo vitreous injection. Animals were reanesthetized the next day, and a separate estimate of rank was obtained. A rank of −3 means that the retinal bleb was apparently flattened. A rank of +3 means that the bleb approximately doubled in size. A 0 rank means that the apparent bleb size was unchanged over time. After all the experiments were completed, the content of each vial was unmasked and compared with the experimenter's conclusions based on the observation of images obtained between 30 and 90 minutes and at 1 day after administration of drug or placebo.

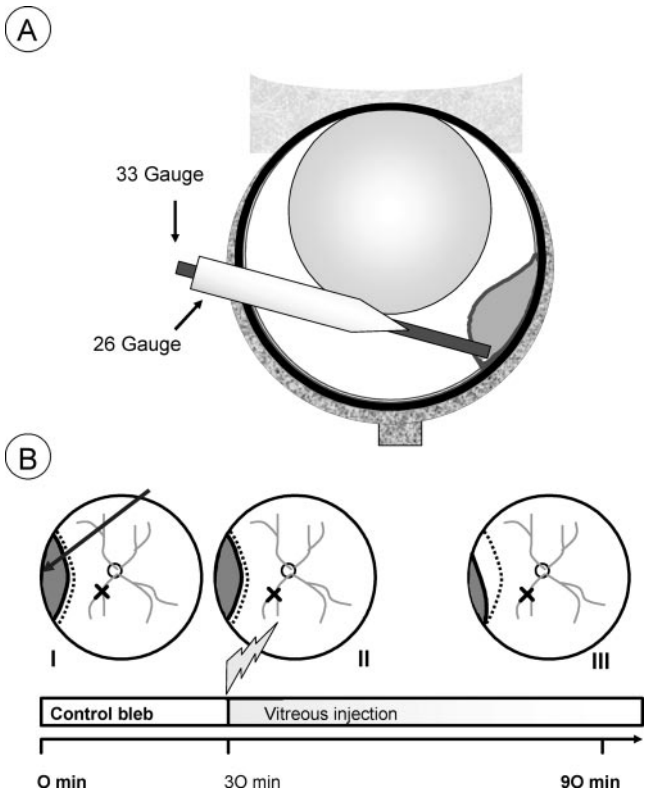

FIGURE 2. (**A**) The rat eye and injection procedure. (**B**) The procedure for tracking the apparent changes in bleb size for control periods (0–30 minutes) and for INS37217-induced changes (30–90 minutes). Panels I, II, and III are three representative time points at which images were obtained during the experiment.

Anesthesia and Physiology

Long-Evans female rats 2 to 2.5 months (200–300 g weight) were anesthetized according to the following protocol: (1) buprenorphine (Buprenex; Reckitt & Colman Pharmaceuticals, Richmond, VA), 0.3 mg/1 mL ampoules, 0.017 mL per 100 g body weight (BW), subcutaneous (SC) injection to reduce animal handling stress and pain reaction; (2) SC injection of pentobarbital sodium 40 minutes later (50

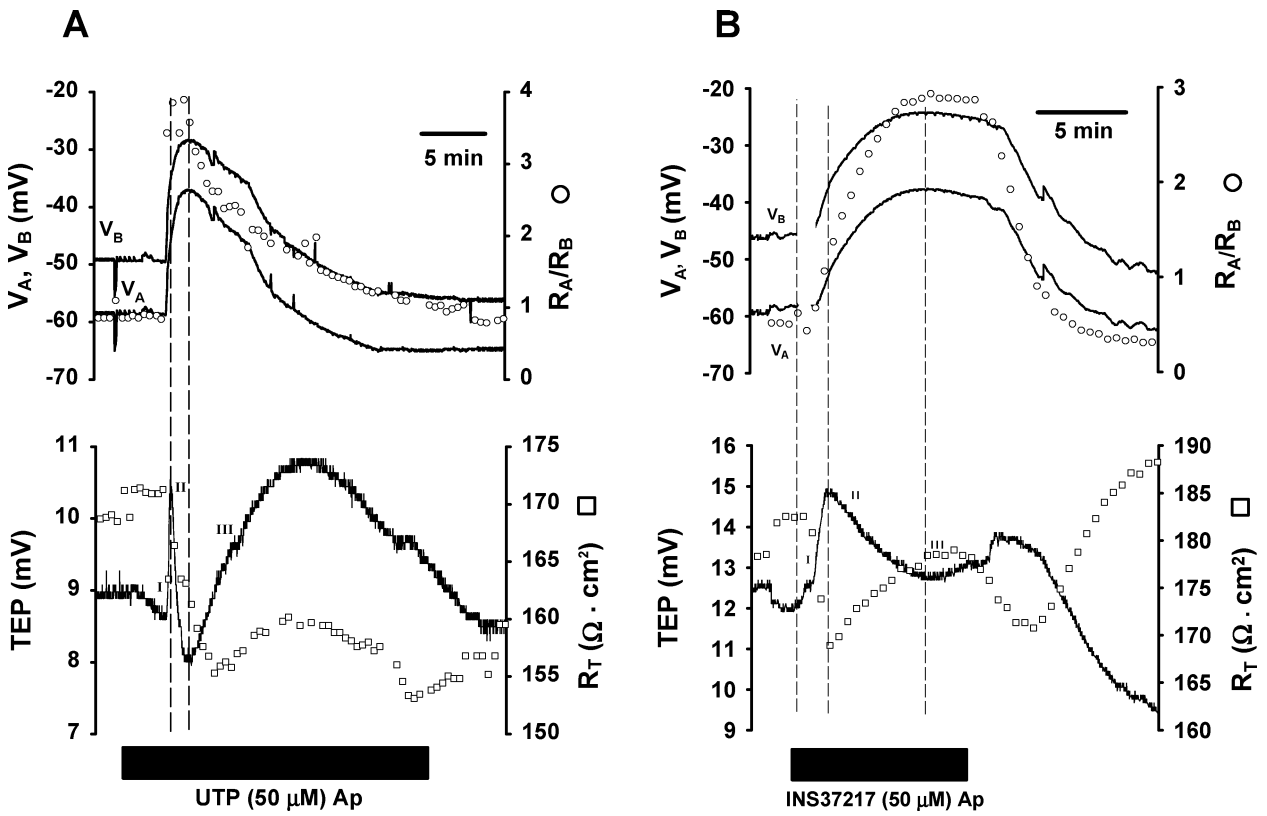

FIGURE 3. (**A**) The voltage and resistance responses of the bovine RPE after the addition of 50 μM UTP to the Ringer's solution perfusing the apical membrane. *Filled rectangle*: length of time UTP was added to the apical chamber. *Top*: *continuous traces* indicate V_A and V_B; *open-circle traces* indicate ratio of apical to basolateral membrane resistance (R_A/R_B). *Bottom*: *continuous trace* is TEP; *open-square trace* denotes transepithelial resistance (R_T). (**A**, **B**, *bottom*, I, II, and III) The components of the triphasic electrical response after the addition of UTP. Phase I was characterized by V_B's depolarizing faster than V_A, which caused an increase in TEP; in addition, R_T decreased and R_A/R_B increased. The start of phase II is operationally defined as the time when TEP first began to decrease, because V_A began to depolarize at a faster rate than V_B. Phase III began when V_A hyperpolarized faster than V_B, producing a slow increase in TEP. During this phase, R_T remained relatively constant, whereas R_A/R_B decreased. (**B**) The voltage and resistance responses of the bovine RPE after the addition of 50 μM INS37217 to the apical bath. Otherwise as in (**A**).

mg/mL; 0.12 mL per 100 g BW; Nembutal, USP; Abbott, Abbott Park, IL); and (3) atropine (50 mg/mL; 0.1 mL per 100 g BW) to reduce lung edema. If the anesthesia was not sufficient, an extra half dose of pentobarbital sodium was injected 40 minutes later. After 15 to 20 minutes, the animal was placed on a heated pad (38°C). Oxygen levels were monitored and kept constant (92%–95%) by using a pulse oximeter (NPB-40; Nellcor). Dehydration was avoided by SC injection of NaCl 0.9% (pH 7.2) solution with 2.5 mM glucose (1 mL per 100 g BW). Animals showing normal physiological blood and urine parameters were used: blood pH 7.1 to 7.4, glucose less than 6.0 mM (glucose levels were normalized in some animals by SC injection), serum osmolarity less than 325 mOsM. The acceptable range of urine parameters were as follows: 0 glucose, protein less than 30 mg/dL, leukocytes: moderate or less (based on Multistix 9 test), negative bilirubin, negative ketones, urobilinogen less than 1 mg/dL, and negative nitrite.

Schematic Diagram of the Preparation

An anesthetized rat was immobilized with ear bars and a nose clip. Body temperature was kept at 35°C to 37°C by a water jacket. Before the vitreous injection procedures, the experimental eye was anesthetized with proparacaine 1% ophthalmic solution, and the iris was dilated with a 1% ophthalmic atropine solution. A specially designed double convex lens, lubricated with carboxymethyl-cellulose (Celluvisc; Allergan, Irvine, CA) eye drops, was placed on the cornea to prevent drying and to increase the visual angle of observation for internal eye structures. The eyelids of the contralateral eye were closed with microserrefine to prevent corneal drying. Using a stereotaxic micromanipulator under stereomicroscope guidance, a 26-gauge guidance needle was inserted into the vitreous chamber, carefully avoiding the lens (Fig. 2A). A 33-gauge blunt needle attached to a syringe (Hamilton, Reno, NV) was inserted into the 26-gauge guidance needle and used to inject drugs into the vitreous and create subretinal blebs. The blebs were created by the 33-gauge needle which was pushed through the guidance needle under visual control until it penetrated the retina while avoiding the RPE. In many cases it was possible to position the 33-gauge needle so that it first penetrated a small retinal blood vessel. Withdrawal of the 33-gauge needle caused a small blood clot that helped seal the retinal hole.

Solutions

Subretinal and vitreal injections were delivered in MPBS solution (13.6 mM Na_2HPO_4, 6.2 mM NaH_2PO_4, 128 mM NaCl, 5 mM KCl) at pH 7.2, osmolarity 285 mOsM. In preliminary experiments, we found that the constancy of apparent bleb size over time depended on the relative osmolarity of the serum and the MPBS solution used in the creation of the subretinal bleb. This observation suggests that in the absence of any perturbation, bleb volume is mainly determined by osmotic differences across the retina and the RPE. Serum osmolarity varied from 295 to 340 mOsM depending on hydration-nutrition levels. Empirically, we found that apparent bleb volume was maintained constant over several hours by setting MPBS solution osmolarity 15 mOsM below the measured serum osmolarity and by setting pH at 7.2. MPBS solution osmolarity adjustments were made by adding mannitol or removing sodium chloride. Fluorescein (0.002%) was used to visualize fluid back leak from the bleb into vitreous.

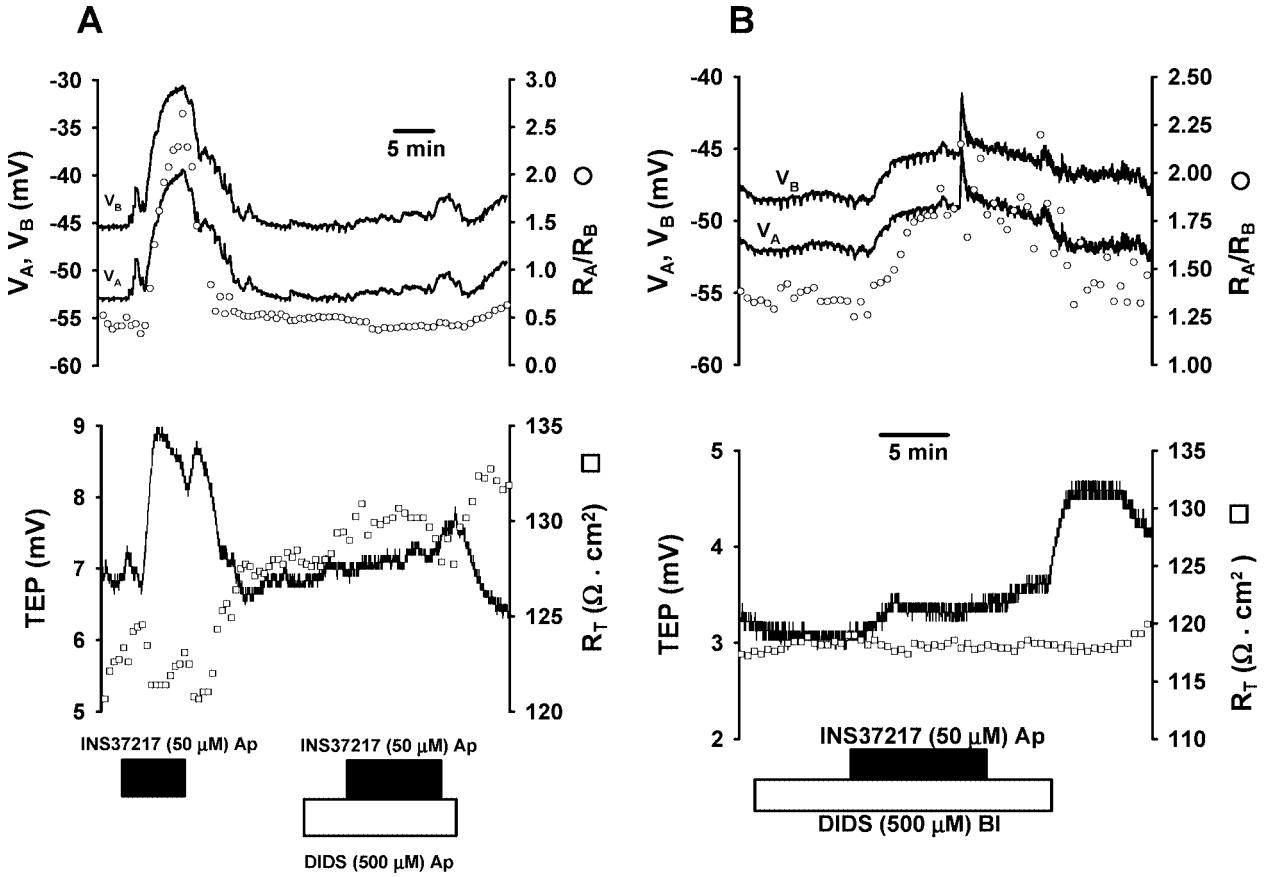

FIGURE 4. (**A**) Effects of apical application of DIDS on the INS37217-induced voltage and resistance responses. *Rectangles*: length of time that indicated compounds were added to the apical chamber. *Top*: *continuous traces* represent V_A and V_B, as labeled; *open-circle traces* are the ratio of apical to basolateral membrane resistance, R_A/R_B. *Bottom*: *continuous trace* is TEP*; open-square trace* denotes transepithelial resistance, R_T. Addition of 50 μM INS37217 to the apical bath caused the usual voltage and resistance changes. The apical membrane was then treated with 500 μM DIDS to block the P2Y/P2U receptors and then 50 μM INS37217 was added to the apical bath in the presence of DIDS. (**B**) The addition of 500 μM DIDS to the basal bath almost completely inhibited the INS37217-induced voltage and resistance responses that were produced in a proceeding control (not shown). Otherwise as in (**A**).

Data Collection and Analysis

An air-cooled digital CCD camera, attached to a stereo microscope (SMZ800; Nikon, Melville, NY), was used to take series of time-lapse images (every minute) over the first 2 hours. The collected images were compared to estimate the changes in apparent bleb size. In Fig. 2B, panel I illustrates the retinal configuration at the time of bleb creation ($t = 0$). Similarly, panels II and III illustrate the retinal configurations at $t = 30$ and 90 minutes, respectively. The maximum observation time during the first day was limited by anesthesia to 4 hours. In the randomized, masked trial experiments, we observed the subretinal bleb for 30 minutes, to point II, before the vitreal injection of placebo or drug. During this initial period there was no leak of fluorescein and no change in apparent bleb size. At point II, after vitreous injection of either placebo or INS37217 we observed the bleb for another 60 minutes. Because the changes in apparent bleb size were monotonic we could use the two images at 30 and 90 minutes to estimate the change in apparent bleb size.

Changes in apparent bleb size were visualized by using a dotted line to mark the bleb border image and an "X" to mark constant reference structures such as the optic nerve or a blood vessel, (Fig. 2B; $t = 0$). By transferring the dotted line along with the fiducial mark we could identify changes in apparent bleb size that occurred over the 90 minutes observation period (Fig. 2B). In each experiment, we also obtained images the next day that were used to strengthen our conclusion about the direction of change in apparent bleb size.

Statistics

Results are expressed as means ± SD unless otherwise indicated. Given the relatively small sample size, we used the nonparametric, Mann-Whitney test for statistical comparisons of unpaired dated and the Wilcoxon signed rank test for paired data.[29,30] $P < 0.05$ is regarded as significant in all comparisons.

RESULTS

Electrophysiological Responses to UTP or INS37217

The experiments summarized in Figs 3A and 3B illustrate near maximal membrane voltage and resistance changes that are produced in bovine RPE when $P2Y_2$ receptor agonists, UTP (50 μM), or INS37217 (50 μM) was added to Ringer's solution in the apical bath. The bottom panels show the changes in TEP (solid trace) and R_T (open-square trace), and the top panels show the changes in V_A and V_B (solid traces) and R_A/R_B (open-circle traces). Before the addition of agonist, the mean V_A and TEP were -55.0 ± 5.1 and 6.6 ± 3.4 mV (mean ± SD; $n = 8$), respectively, and the mean R_T and R_A/R_B were 145 ± 31 $\Omega(cm^2)$ and 0.7 ± 0.6, respectively.

After addition of UTP or INS37217, the TEP and membrane voltages underwent three distinct phases with onset times

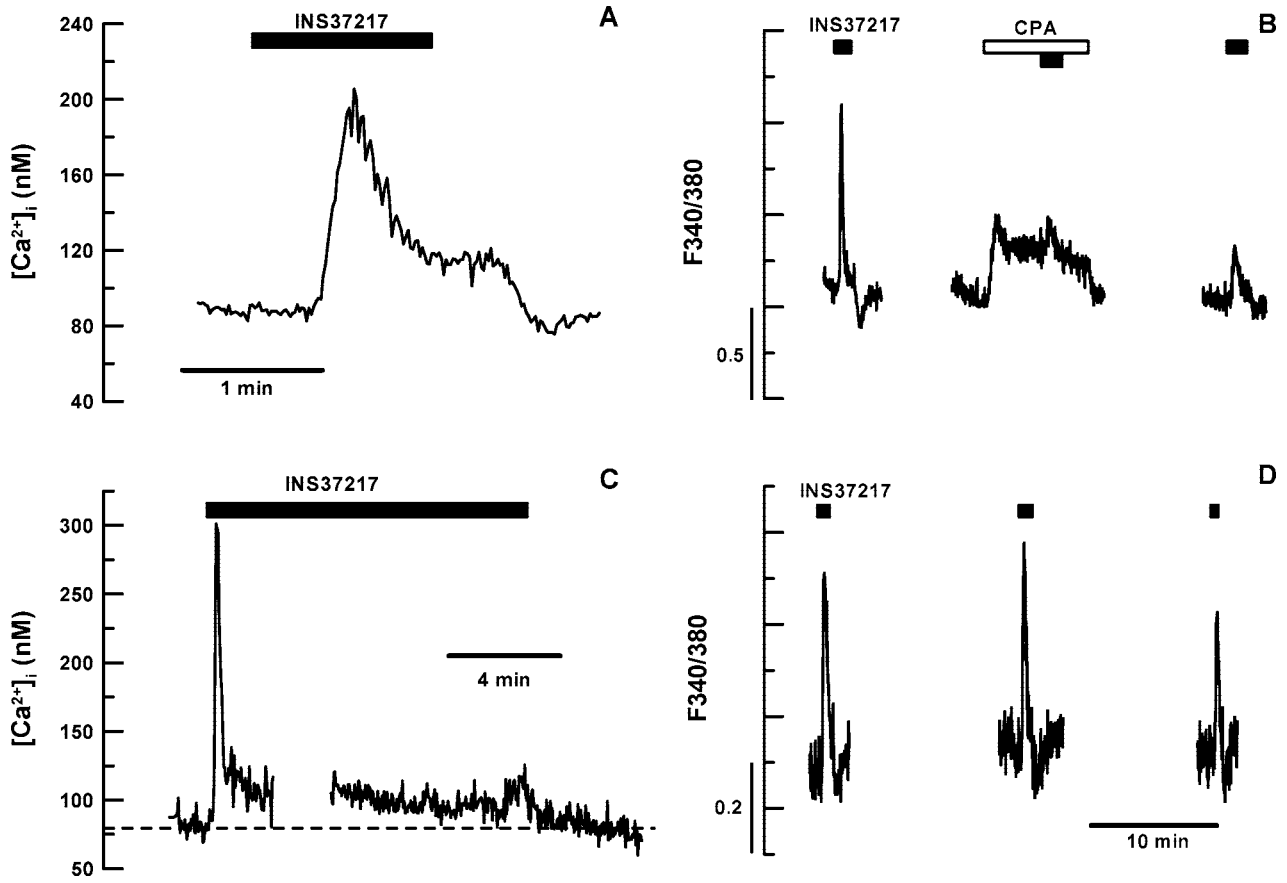

FIGURE 5. (**A**) Effect of INS37217 on $[Ca^{2+}]_i$. INS37217 (100 μM) was applied apically for approximately 90 seconds (*filled rectangle*), and caused a rapid, transient increase in $[Ca^{2+}]_i$. (**B**) Effect of CPA on the INS37217-induced changes in $[Ca^{2+}]_i$. Apical INS37217 caused a transient increase in the F340/F380 ratio (*left trace*), indicating an increase in $[Ca^{2+}]_i$. Apical CPA (5 μM), an ER Ca^{2+}-ATPase blocker, caused a transient increase in F340/F380, followed by a steady state elevation above baseline (*middle trace*). In the presence of CPA, the INS37217-induced ratio increase was approximately 10% of the control response. Apical INS37217 increased the F340/F380 ratio approximately 30% of control, indicating that inhibitory effect of CPA was partially reversible (*right trace*). This experiment took place over 34 minutes. (**D**) Control experiment on another tissue from the same eye showed that repeated application of INS37217 over 34 minutes caused a very similar increases in F340/F380. The first two additions of INS37217 were for approximately 1 minute, and the third addition was for 30 seconds. (**C**) Effect of prolonged addition of INS37217 on $[Ca^{2+}]_i$. INS37217 (100 μM) was applied apically for approximately 12 minutes (*filled rectangle*). INS37217 caused a rapid, transient increase in F340/F380, followed by sustained elevation of $[Ca^{2+}]_i$ above the baseline levels (F340/F380). Removal of INS37217 from the apical bath decreased in F340/F380 to baseline.

labeled I, II, and III.[31] During phase I, the TEP increased because V_B depolarized faster than V_A; in addition R_T decreased and R_A/R_B increased, consistent with an decrease in R_B. The voltage and resistance changes during phase I are consistent with an increase in basolateral membrane Cl conductance.[20,32] In three experiments, similar to Fig. 3A, the mean UTP-induced depolarization of V_A was 22.5 ± 0.5 mV during phase I, which increased TEP by 2.5 ± 0.7 mV. Concomitantly, the decrease in R_T was 17.7 ± 7.6 $\Omega(cm^2)$ while R_A/R_B increased by 2.3 ± 0.9.

The INS37217-induced changes in phase I (Fig. 3B) were not significantly different in magnitude from the UTP-induced changes ($P > 0.5$, Mann-Whitney test). In five experiments, the mean INS37217-induced depolarization of V_A was 16.0 ± 4.0 mV during phase I, which increased TEP by 3.8 ± 2.0 mV. Concomitantly, the decrease in R_T was 10 ± 4 $\Omega(cm^2)$ while R_A/R_B increased by 1.6 ± 0.7. In six experiments, we compared the magnitude of the INS37217- and UTP-induced phase I changes in TEP as a function of concentration. At 1, 10, and 25 μM ($n = 3$), there was no significant difference ($P > 0.5$, Wilcoxon signed rank test) but at 50 and 100 μM ($n = 6$ and 4), respectively, the INS37217 responses were significantly ($P < 0.01$) larger than the comparable UTP responses.

The transition between phases I and II occurred when the TEP peaked and began to decrease. During phase II, R_T and R_A/R_B increased, and V_A depolarized faster than V_B. These phase II changes are more clearly seen in Figure 3B and are consistent with a decrease in apical membrane conductance. Approximately 90% of this conductance is due to Ba^{2+}-sensitive K channels,[23] suggesting that the closure of K channels is a major contributor to the phase-II voltage changes.[20] Phase III is operationally defined as the time point at which TEP began to increase again. During phase III, TEP increased because V_A hyperpolarized at a faster rate than V_B; in addition, R_A/R_B slowly decreased and R_T first decreased and then increased. These phase III electrical effects were relatively small, variable in time course, and difficult to study.

Effect of Apical or Basolateral Application of DIDS on INS37217-Induced Electrical Responses

Previous work has shown that micromolar amounts of apical 4,4′-diisothiocyanatostilbene-2,2′-disulfonic acid (DIDS) inhibits P2Y receptors in a variety of cell types, including bovine RPE.[20,33–36] To determine whether the INS37217-mediated electrical effects can be inhibited by apical application of DIDS,

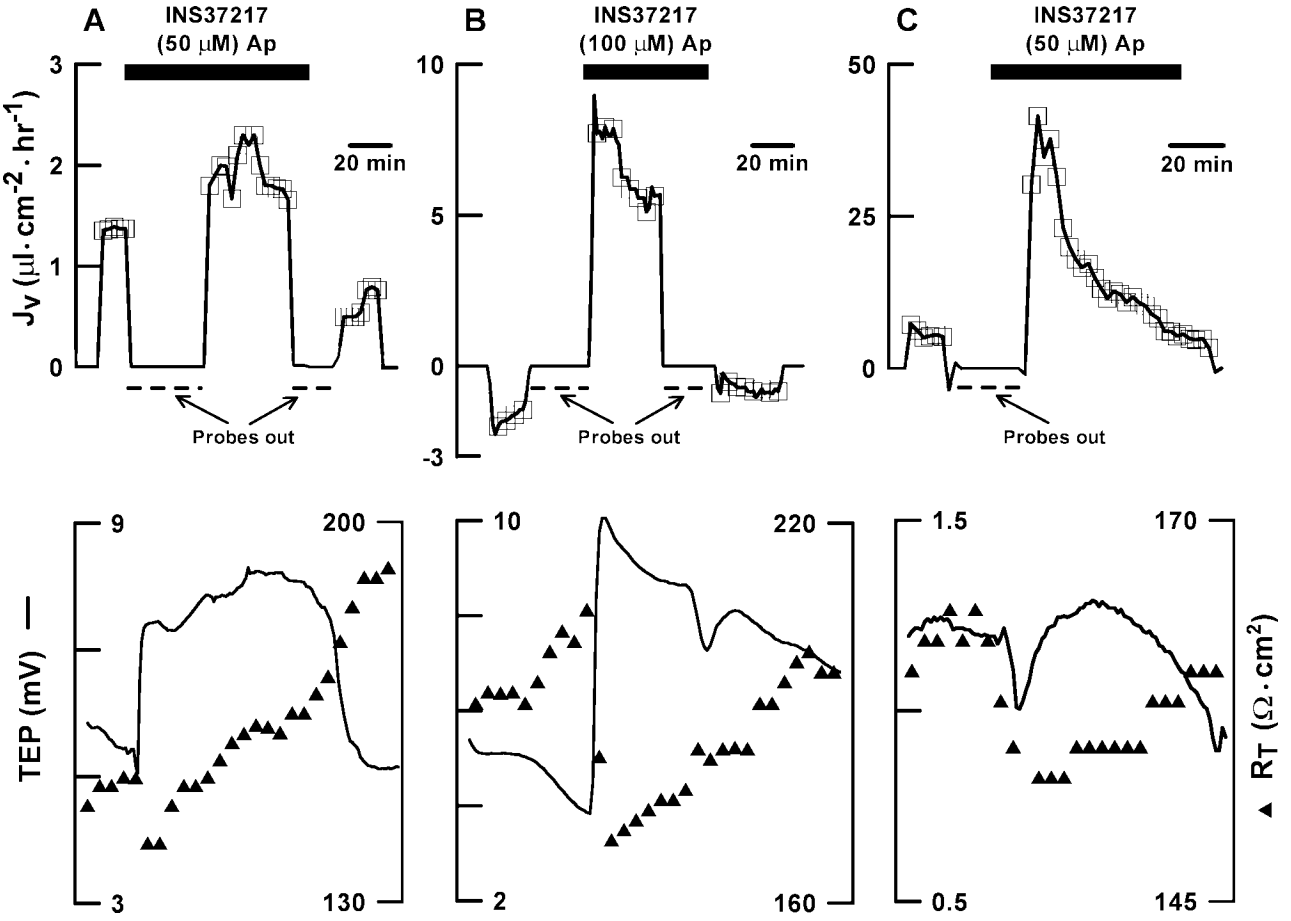

FIGURE 6. (**A**) Net fluid absorption (J_V) increased after addition of 50 μM INS37217 to the apical bath of bovine RPE. *Top*: J_V across bovine RPE in the absence and presence of INS37217; *bottom*: TEP and R_T measurements. In control Ringer's solution, fluid was absorbed at a rate of ≈1.3 μL/cm^2 per hour. Addition of 50 μM INS37217 to the apical bath reversibly increased J_V to ≈2.1 μL/cm^2 per hour. TEP increased and R_T decreased as expected for an INS37217. (**B**) Net fluid transport (J_V) was reversed from secretion, approximately −2.8 μL/cm^2 per hour in control Ringer, to absorption, ≈5.0 μL/cm^2 per hour, after addition of 100 μM INS37217 to the apical bath of bovine RPE. (**C**) INS37217 (50 μM) was added to the solution bathing the apical membrane of native fetal human RPE after the obligatory control-to-control changes (not shown). INS37217 elicited a large transient increase in J_V followed by a slow 68-minute decrease to a steady state level of approximately 5.0 μL/cm^2 per hour, the original control level.

INS37217 was added to apical Ringer's solution in the absence or presence of DIDS. Figure 4A shows that in the presence of 500 μM apical DIDS, the electrical effects of INS37217 were almost completely abolished. In the presence of DIDS, the mean ± SD of INS37217-induced changes in V_A, TEP, R_T, and R_A/R_B were all reduced by at least a factor of five compared to control values: 2.4 ± 3.1 and 0.2 ± 0.2mV, 0.2 ± 0.4 Ω(cm^2), and 0.3 ± 0.4, respectively (n = 5).

Previous work in bovine RPE has demonstrated that the addition of 500 μM DIDS to the basolateral bath specifically blocks basolateral membrane Cl conductance without altering K conductance.[23,37,38] If phase I of the INS37217-induced electrical responses is due to an increase in basolateral membrane Cl conductance, as suggested earlier, then the effects of INS37217 should be blocked by addition of DIDS to the basolateral bath. This notion was confirmed in the experiment shown in Fig. 4B, in which 500 μM DIDS clearly inhibited the effects of apical INS37217. This result was confirmed in two other experiments. The findings shown in Figures 4A and 4B provide strong pharmacologic evidence that the effects of INS37217 are mediated by activation of the $P2Y_2$ receptor at the apical membrane and a subsequent increase in basolateral membrane Cl conductance.

Role of $[Ca^{2+}]_i$

In many systems, agonist induced activation of $P2Y_2$ receptors has been shown to increase IP3–mediated release of Ca^{2+} from the endoplasmic reticulum (ER).[2,39–41] The downstream effects of activation of the $P2Y_2$ receptor can be blocked by pharmacologically unloading Ca^{2+} from ER stores with inhibitors of sarco-endoplasmic reticulum Ca^{2+} adenosine triphosphatase (ATPase) (SERCA).[20] Figure 5A shows that 100 μM apical INS37217 transiently increased $[Ca^{2+}]_i$ from 80 to 200 nM. In 10 experiments, INS37217 increased $[Ca^{2+}]_i$ by 101 ± 14.4 nM (mean ± SEM) from a baseline of 89.5 ± 14.4 nM. These INS37217-induced effects on $[Ca^{2+}]_i$ are consistent with $P2Y_2$ receptor–mediated signaling through the PLC-β pathway.

If the INS37217-induced increase in $[Ca^{2+}]_i$ is due to $P2Y_2$ receptor activation, then these effects of INS37217 should be inhibited by cyclopiazonic acid (CPA), which blocks SERCAs and unloads ER Ca^{2+} stores.[42,43] Figure 5B summarizes a series of three consecutive 100 μM INS37217–induced $[Ca^{2+}]_i$ responses that were obtained over a period of 40 minutes, either in the absence or presence of 5 μM apical CPA. The control response (Fig. 5B, left trace) shows a typical increase in $[Ca^{2+}]_i$ in the presence of apical INS37217. Pretreatment with CPA dramatically inhibited the INS37217-induced $[Ca^{2+}]_i$ response

(middle trace), which did not recover even after CPA washout (right trace). Fig. 5D shows a control experiment in which three consecutive additions of INS37217 (100 μM), also over a 40 minute period but in the absence of CPA, produced relatively similar consecutive $[Ca^{2+}]_i$ responses. The third response (right trace) was approximately half the duration of the first two responses and consequently was reduced in size. The results illustrated in Fig. 5D show that the CPA-induced blockade of the INS37217-mediated $[Ca^{2+}]_i$ responses shown in Fig. 5B were not due to receptor desensitization or downregulation of the $P2Y_2$-receptor signaling pathway that may have resulted from mere repeated additions of INS37217 to the same tissue.

To determine whether INS37217 produced long term, steady state increases in $[Ca^{2+}]_i$, we treated the apical membrane with Ringer's solution containing 100 μM INS37217 for 12 minutes while continuously monitoring $[Ca^{2+}]_i$. Fig. 5C shows that INS37217 produced a typical transient increase in $[Ca^{2+}]_i$. A small elevation in baseline $[Ca^{2+}]_i$ (0.4 ratio units or 23% of the transient increase) was maintained for as long as the agonist was present in the apical bath. This result was obtained in three experiments and suggests that apical INS37217 can cause sustained alterations in intracellular Ca^{2+} signaling in RPE.

INS37217-Induced Changes in Fluid Transport across Bovine and Human RPE

In these experiments TEP, R_T, and net fluid transport (J_V) were measured in the absence or presence of INS37217 in the apical bath. Fig. 6A shows that before the addition of 50 μM INS37217, the RPE absorbed fluid at approximately 1.3 μL/cm^2 per hour. TEP was 5.5 mV, and R_T was 153 Ω(cm^2). The addition of INS37217 (50 μM) to the apical bath increased TEP to 8 mV and decreased R_T to 141 Ω(cm^2). In addition, J_V increased to approximately 2.0 μL/cm^2 per hour. The TEP and J_V changes were reversible and lasted as long as the agonist was applied. In 13 tissues, the mean values of TEP, R_T, J_V were 7.5 $\pm$ 0.4 mV, 173 $\pm$ 11 Ω(cm^2), and 1.6 $\pm$ 0.3 μL/cm^2 per hour (mean $\pm$ SEM), respectively. After the addition of 50 μM INS37217 to the apical bath, TEP increased by 2 mV to 9.7 $\pm$ 0.7 mV ($P < 0.005$), R_T decreased to 163 $\pm$ 9 Ω(cm^2) ($P < 0.001$) and mean fluid absorption increased by more than a factor of two, to 3.8 $\pm$ 0.6 μL/cm^2 per hour ($P < 0.02$).

In some bovine tissues, net fluid transport in control conditions was in the secretory direction. One such example is shown in Fig. 6B. Initially, J_V was approximately -2.8 μL/cm^2 per hour and the addition of INS37217 to the apical bath increased net fluid absorption to approximately 7 μL/cm^2 per hour. The TEP and R_T changes were very similar to those shown in Fig. 6A (and Fig. 3B). Fig. 6C illustrates the effects of INS37217 on electrical and fluid transport parameters in native human fetal RPE.[32] In the absence of agonist, J_V was approximately 5.0 μL/cm^2 per hour. INS37217 (50 μM) was then added to the apical bath and caused a relatively small but rapid increase in TEP, a concomitant decrease in R_T (20 Ω(cm^2), and a large increase in J_V to approximately 40 μL/cm^2 per hour that declined over the following 50 minutes back to the baseline of 5.0 μL/cm^2 per hour. This result suggests that INS37217 can stimulate ion and fluid transport in human tissues.

To test if the INS37217-induced increase in $[Ca^{2+}]_i$ is associated with the observed stimulation of fluid transport, we evaluated the effects of INS37217 on J_V in the absence and presence of CPA. Because CPA was shown to inhibit the INS37217-induced increase in $[Ca^{2+}]_i$, we expect that pretreatment with CPA would also inhibit the INS37217-mediated increase in J_V. This expectation was confirmed in the experiment summarized in Fig. 7A. Addition of CPA (5 μM) to the apical bath increased J_V from 1 to approximately 3.8 μL/cm^2 per hour, which may be attributed to a CPA-induced increase in $[Ca^{2+}]_i$ (see Fig. 5B), resulting in an increase in basolateral membrane Ca^{2+}-sensitive Cl conductance and a concomitant increase in apical-to-basolateral fluid transport.[26,44,45] In the presence of CPA, the addition (or removal) of 100 μM apical INS37217 produced no change in J_V. In three experiments, in the presence of CPA plus INS37217, J_V was 3.5 $\pm$ 1.2 μL/cm^2 per hour, not significantly different from CPA alone (4.1 $\pm$ 1.4 μL/cm^2 per hour; mean $\pm$ SEM). Apical DIDS, which is a putative antagonist for the $P2Y_2$ receptor, was shown to block INS37217-mediated electrophysiological effects (Fig. 4A). Therefore, we expected that apical DIDS should also block the INS37217-induced changes in J_V. Fig. 7B is one of three similar experiments that compared the INS37217–induced changes in J_V, in the absence and presence of apical DIDS (500 μM). In the control response, 100 μM INS37217 was added to the apical bath and transiently increased J_V from approximately 1 to 4 μL/cm^2 per hour. These responses were reversible. Apical DIDS (500 μM) produced no appreciable changes in J_V. There was no effect of INS37217 on J_V in the presence of 500 μM DIDS. In three experiments, in the presence of DIDS plus INS37217 J_V was 1.9 $\pm$ 0.8 μL/cm^2 per hour, not significantly different from DIDS alone (1.5 $\pm$ 0.1 μL/cm^2 per hour). The results shown in Figures 7A and 7B strongly suggest that the INS37217-induced increases in net fluid absorption across RPE are mediated by activation of apical membrane P2 receptors and ER release of Ca^{2+}.

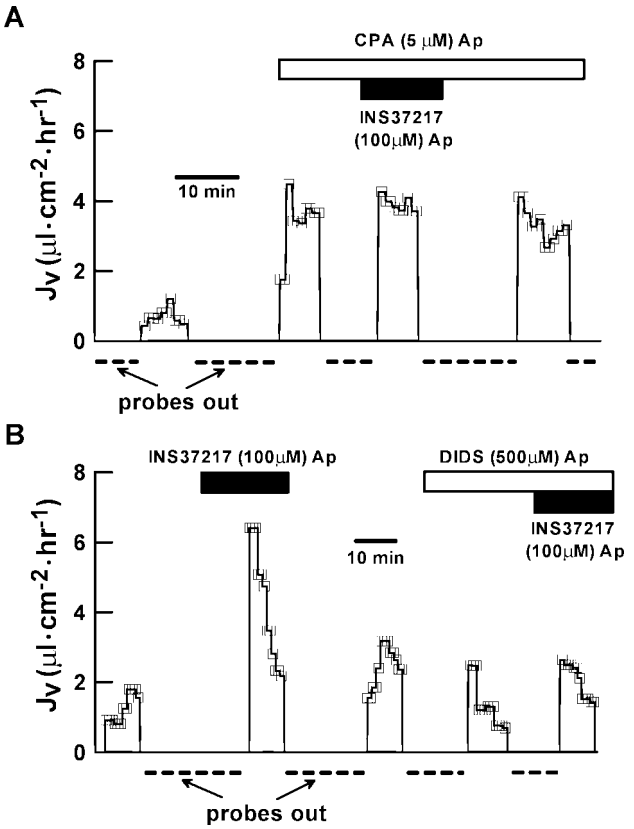

FIGURE 7. (**A**) CPA blocks the INS37217-induced increase in J_V. In a control response (not shown), 100 μM apical INS37217 increased J_V, from 4 to 7 μL/cm^2 per hour but the following control was 1 μL/cm^2 per hour. Apical CPA increased J_V from 1 to 3.8 μL/cm^2 per hour. In the presence of CPA, the addition (or removal) of 100 μM apical INS37217 produced no change in J_V. (**B**) Apical DIDS blocked the INS37217-induced increase in J_V. In the presence of DIDS, the addition (or removal) of 100 μM apical INS37217 produced no change in J_V.

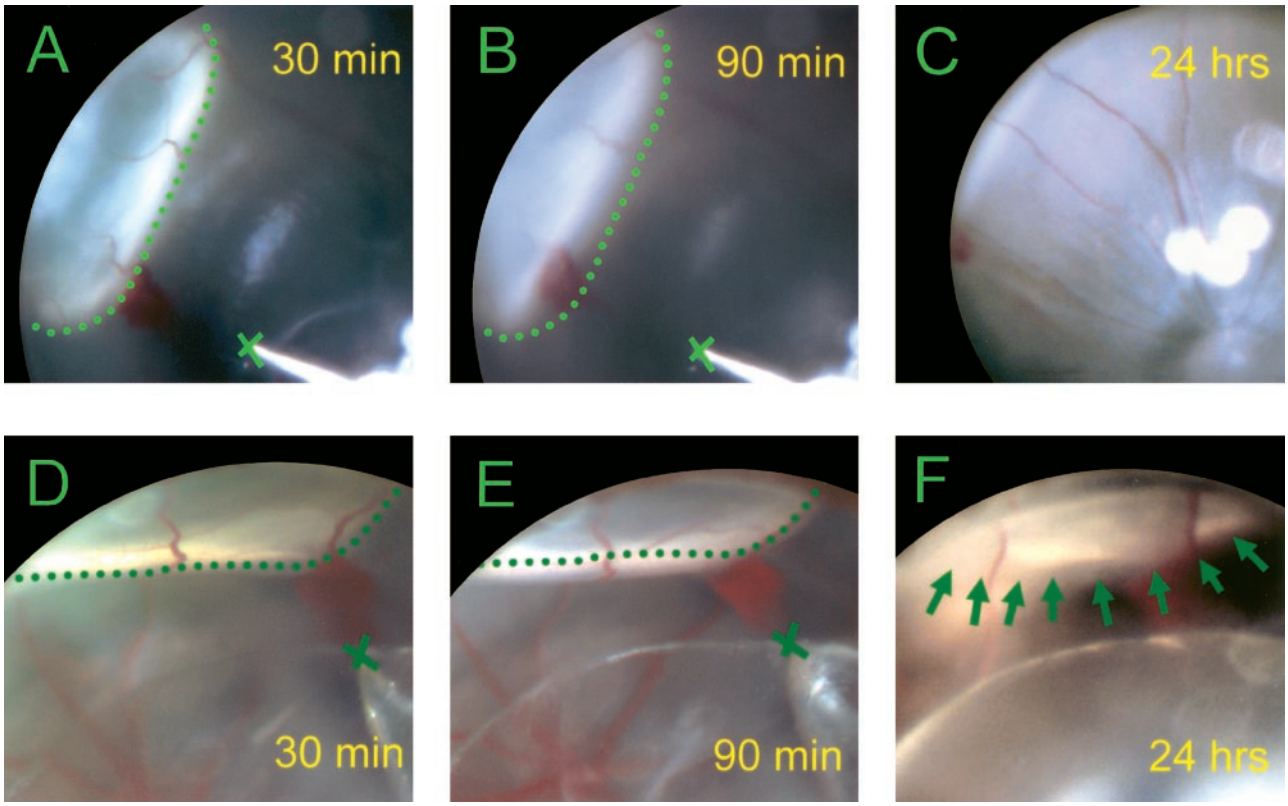

FIGURE 8. INS37217-induced bleb volume changes in the intact rat eye. Drug injected animal: (**A**, *dotted line*) Apparent bleb size after a 30-minute control period. At 30 minutes, 3 μL of 5 mM INS37217 Ringer was injected into the vitreous. (**B**) The apparent bleb size 60 minutes after the injection of the drug (t = 90 minutes). For comparison, the *dotted line* from (**A**) was transferred to (**B**). After the same animal was reanesthetized the next day, image (**C**) was obtained, which shows that the bleb was completely flattened 24 hours after the injection of INS37217 into the vitreous. Control-injected animal: (**D**, *dotted line*) Apparent bleb size after a 30-minute control period. At 30 minutes, 3 μL control solution was injected into the vitreous. Image (**E**) shows the apparent bleb size 60 minutes after the injection of placebo solution (t = 90 minutes). For comparison, the *dotted line* from (**D**) was transferred to (**E**). The same animal was reanesthetized the next day, image (**F**) was obtained, which shows that the bleb was still present.

Effects of Intravitreal INS37217 on Subretinal Blebs

Figure 8 compares two sets of time-lapse video fundus images from experimentally produced subretinal blebs, one from an eye with intravitreally administered INS37217 (Figs. 8A–C), and the other from an eye injected intravitreally with control Ringer's solution (Figs. 8D–F). At the 30-minute time point, 3 μL of either INS37217-containing (5 mM) Ringer's solution or control Ringer's solution was injected into the vitreous, and each subretinal bleb was observed for another 60 minutes. At 90 minutes, the INS37217-treated eye showed a small decrease in apparent bleb size, whereas the control eye showed a small increase in apparent bleb size. In the INS37217-treated eye, the experimentally produced bleb was not present the next day indicating that the retina had flattened. In contrast, the subretinal bleb remained essentially unchanged in the control eye. This experiment suggests that vitreous injection of INS37217 can effectively reduce the volume of experimentally produced retinal detachments in the rat eye.

Twelve similar experiments (1 eye per rat) were performed in a masked fashion to provide a rigorous and objective evaluation of the effects of INS37217 on fluid reabsorption from experimentally produced subretinal blebs. In these experiments, after the creations of blebs, drug or placebo solutions were injected into vitreous of the rat eye in a masked fashion (vials and their contents were indistinguishable). After all 12 eyes were scored, the key was unmasked and compared with the summarized results based on the observations at 1 and 24 hours. The results summarized in Figure 9B show a significant difference ($P < 0.005$) between INS37217 (filled bars) and vehicle control (placebo, unfilled bars) on the scoring of subretinal blebs. After one hour of treatment, the INS37217-treated eyes all showed a decrease in bleb size, whereas the control eyes all showed an increase in bleb size. The next day, the subretinal blebs from the INS37217-treated eyes had almost completely disappeared, whereas the subretinal blebs from the vehicle-treated eyes remained essentially unchanged. In four of six INS37217-treated eyes, the retina appeared completely flat at the 24-hour time point. (UTP and INS37217 produce similar physiological responses in vitro [see Fig. 3] but different responses in vivo. In contrast to the results with INS37217, vitreous injection of the same amount of UTP, under identical experimental conditions [n = 5, data not shown], produced no visible decrease in apparent bleb size at 1 and 24 hours. This result shows that an effective dose of UTP could not be achieved at the apical membrane of the RPE, suggesting that intravitreal UTP was degraded in its diffusion to the SRS.)

DISCUSSION

The RPE apical membrane is a potential target for therapeutic small molecules that bind membrane receptors, alter second-messenger activity, and activate ion transport-coupled fluid absorption from the SRS. Previous in vitro work has shown that the apical membrane of the RPE contains $P2Y_2$ receptors that are activated by endogenous nucleotides such as ATP and UTP,

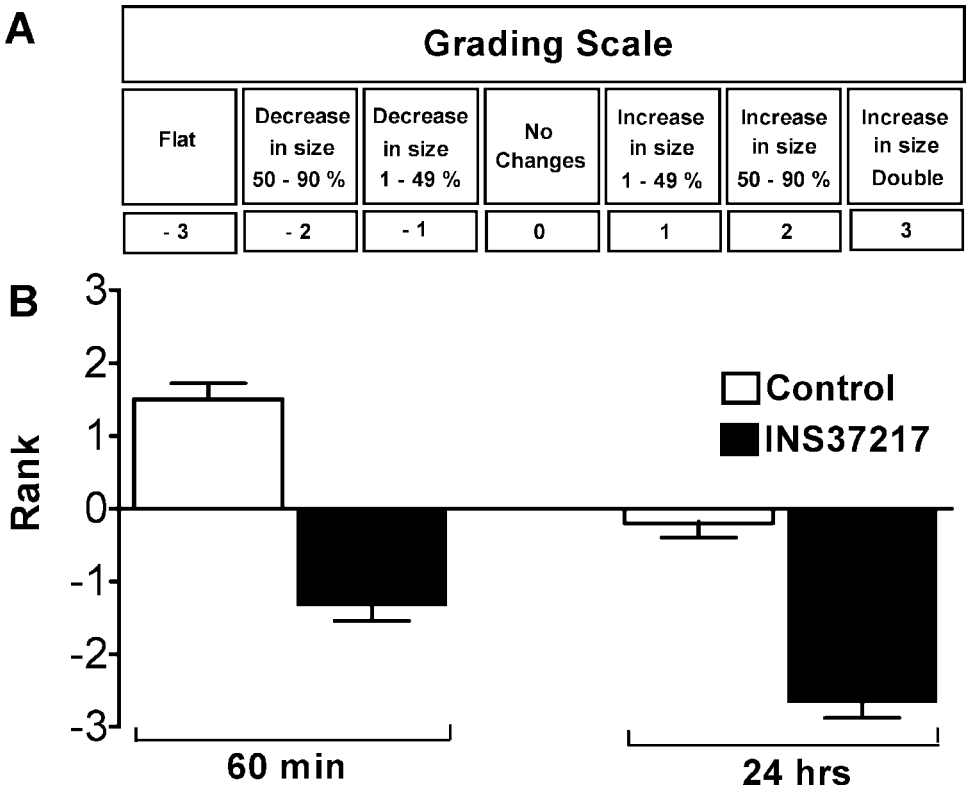

FIGURE 9. (**A**) Grading scale for masked trial experiments. (**B**) Mean results of 12 masked-trial experiments. Data are the mean placebo and INS37127 injection vitreous data. The mean ± SEM of the estimated rank for placebo and INS37217 experiments are plotted at 60 minutes and 24 hours. At both 60 minutes and at 24 hours, the mean of the placebo and INS37217 data are significantly different ($P < 0.005$; two-tailed Mann-Whitney test).

which lead to an increase in cytosolic Ca^{2+} levels, and the stimulation of active ion-coupled apical-to-basolateral membrane fluid transport.[20] This increase in fluid transport is most likely generated by an increase in net Cl and K absorption across the epithelium, the latter by blockade of K recycling at the apical membrane (Fig. 3B, phase II) and the former by activation of Ca^{2+}-sensitive Cl channels at the basolateral membrane (Fig. 3B, phase I).[32,37,44–46] The schematic diagram shown in Figure 10 summarizes the plasma membrane transport proteins, receptors, and intracellular signaling pathways that mediate fluid flow across the RPE.

These in vitro findings suggest that activation of $P2Y_2$ receptors in vivo may stimulate subretinal fluid reabsorption. To evaluate the effects of $P2Y_2$ receptor activation in vivo appropriately, we used a hydrolysis-resistant, synthetic $P2Y_2$ receptor agonist, INS37217 in a series of in vitro and in vivo studies. The objectives of the in vitro studies were to use freshly isolated monolayers of bovine or human fetal RPE to confirm that INS37217 produced $[Ca^{2+}]_i$ and electrophysiological effects that were similar to those of UTP and to further characterize the pharmacologic and physiological responses of the RPE to $P2Y_2$ receptor activation. The objectives of the in vivo component of these studies were to determine and compare the effects of intravitreally administered INS37217 and UTP in stimulating subretinal fluid reabsorption in a rodent model of induced retinal detachment.

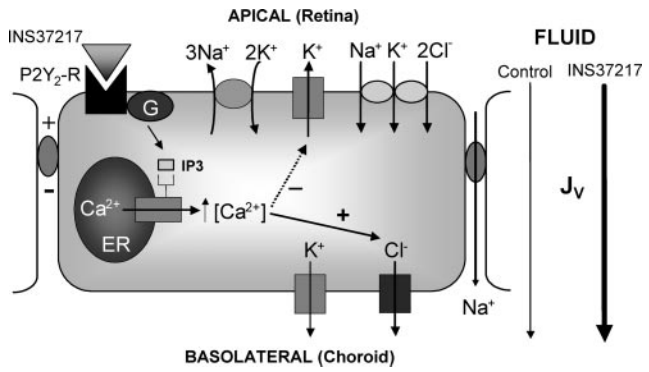

FIGURE 10. A summary of some of the known effects of INS37217 on RPE physiology. Apical INS37217 activates the G-protein–coupled $P2Y_2$ receptor, which in other systems is linked by heterotrimeric G proteins to intracellular PLC, thus generating production of IP3 and a subsequent efflux of Ca^{2+} from intracellular stores. Elevation of cytosolic Ca^{2+} leads to an increase in basolateral membrane Cl conductance, a decrease in apical membrane K conductance, and stimulation of net apical-to-basolateral fluid absorption.

Our results show that constitutive addition of INS37217 to Ringer's solution bathing the apical membrane of bovine RPE produced a large, transient increase in $[Ca^{2+}]_i$, which was followed by a modest, sustained elevation of $[Ca^{2+}]_i$ in the presence of the agonist. INS37217 elicited changes in membrane voltages and resistances were similar in characteristics to those elicited by UTP. INS37217 also increased fluid absorption in the apical-to-basolateral direction in bovine and human fetal RPE monolayers; and, in fluid-secreting bovine RPE, it reversed the direction of fluid transport. In addition, INS37217-induced increases in fluid transport were blocked by apical DIDS in vitro (Fig. 7B) and in vivo ($n = 4$, not shown), after its injection into the bleb. Both results indicate that INS37217 had its main effect at the RPE apical surface. In an experimental model of retinal detachment in rat, intravitreal injection of INS37217, but not UTP, enhanced subretinal fluid reabsorption and retinal reattachment. These in vivo findings strongly suggest that intravitreal UTP is degraded before diffusing to the RPE apical membrane and underscore the necessity of developing an intravitreally administered, hydrolysis-resistant P2 receptor agonist to stimulate subretinal fluid reabsorption in vivo.

Physiological Implications

Accumulation of fluid in the SRS is a hallmark of all clinical retinal detachments, and a mechanism to facilitate net fluid efflux out of this space may be clinically useful to reattach the retina.[47] Pharmacologic enhancement of the RPE pump to reabsorb extraneous subretinal fluid therefore represents a potential approach for inducing reattachment of the retina in the clinic. From the present in vitro bovine RPE experiments we determined that 50 μM INS37217 increased J_V by 2 μL/cm^2 per hour. If this increase occurred over the entire surface of the RPE (approximately 5 cm^2),[48] it would result in the removal of approximately 0.25 mL/d, a clinically significant amount.[49] In the in vitro experiment using native human RPE (Fig. 6C) addition of 50 μM INS37217 to the apical bath kept J_V elevated above baseline for more than 60 minutes. The area under this curve is the total volume transported per unit area. If this transport (approximately 17 μL/cm^2) took place across the back of an adult human eye (approximately 5 cm^2) it would cause the removal of 0.085 mL/h or 2 mL/d.

In addition, the in vivo data allowed us to make a similar calculation using the intact rat eye. Bleb volume changes were calculated by assuming that the bleb formed an ellipsoid of revolution, where $V = 4/3 \cdot \pi \cdot a \cdot b \cdot h$, where a and b are semimajor and semiminor axes, respectively, h is a height of the bleb, and $a = b$ (spread of fluid is isotropic in the plane of the retina). The percentage of volume change was calculated by measuring the number of pixels along the a and b dimensions at $t = 0$ and $t = 60$ minutes: $V_{60}/V_0 = (2/3 \cdot \pi \cdot a^2 \cdot h)_{60}/(2/3 \cdot \pi \cdot a^2 \cdot h)_0$. We used this ratio and the initially injected volume to estimate the mean INS37217-induced change, which was 1.04 $\pm$ 0.5 μL/h (mean $\pm$ SD, n =5). In a typical experiment, a 3 μL injection formed a circular cross-section on the retina of 2 mm diameter (0.03-cm^2 area) The INS37217-induced efflux rate through this area would be 32 μL/cm^2 per hour.

Vitreous injection of the hydrolysis resistant INS37217 could activate the entire surface of the RPE, which would cause the removal of an extra 3.8 mL/d, assuming an efflux rate of 32 μL/cm^2 per hour over the entire area of the RPE. This could be an overestimate of the RPE contribution if the entire RPE area were not activated or if some of the extra fluid exited by a different pathway (e.g., the ciliary body). Nevertheless, based on these extrapolated analyses of the present in vitro and in vivo data, our findings strongly suggest that stimulation of RPE fluid pump function by INS37217 represents a reasonable approach for removing abnormally accumulated subretinal fluid associated with retinal detachments.

Acknowledgments

The authors thank Andy Graham for providing the design of the masked trial.

References

1. Ralevic V, Burnstock G. Receptors for purines and pyrimidines. *Pharmacol Rev.* 1998;50:413–492.
2. Dubyak GR. Signal transduction by P2-purinergic receptors for extracellular ATP. *Am J Resp Cell Mol Biol.* 1991;4:295–300.
3. Yerxa BR, Johnson FL. $P2Y_2$ receptor agonists: structure, activity, and therapeutic utility. *Drugs Future.* 1999;24:759–769.
4. Bringmann A, Pannicke T, Moll V, et al. Upregulation of P2X receptor currents in Muller glial cells during proliferative vitreoretinopathy. *Invest Ophthalmol Vis Sci.* 2001;42:860–867.
5. Fujihara T, Murakami T, Fujita H, Nakamura M, Nakata K. Improvement of corneal barrier function by the P2Y agonist INS365 in a rat dry eye model. *Invest Ophthalmol Vis Sci.* 2001;42:96–100.
6. Cha SH, Hahn TW, Sekine T, Lee KH, Endou H. Purinoceptor-mediated calcium mobilization and cellular proliferation in cultured bovine corneal endothelial cells. *Jpn J Pharmacol.* 2000;82:181–187.
7. Wheeler-Schilling TH, Marquordt K, Kohler K, Jabs R, Guenther E. Expression of purinergic receptors in bipolar cells of the rat retina. *Brain Res Mol Brain Res.* 2000;76:415–418.
8. Hosoya K, Ueda H, Kim KJ, Lee VH. Nucleotide stimulation of Cl(−) secretion in the pigmented rabbit conjunctiva. *J Pharmacol Exp Ther.* 1999;291:53–59.
9. Merriman-Smith R, Tunstall M, Kistler J, et al. Expression profiles of P2-receptor isoforms P2Y1 and P2Y2 in the rat lens. *Invest Ophthalmol Vis Sci.* 1998;39:2791–2796.
10. Sullivan DM, Erb L, Anglade E, et al. Identification and characterization of P2Y2 nucleotide receptors in human retinal pigment epithelial cells. *J Neurosci Res.* 1997;49:43–52.
11. Shahidullah M, Wilson WS. Mobilisation of intracellular calcium by P2Y2 receptors in cultured, non-transformed bovine ciliary epithelial cells. *Curr Eye Res.* 1997;16:1006–1016.
12. Pederson JE. Fluid physiology of the subretinal space. In: Wilkinson CP, ed. *Retina.* St. Louis: Mosby; 1994:1955–1968.
13. Hughes BA, Gallemore RP, Miller SS. Transport mechanisms in the retinal pigment epithelium. In: Marmor MF, Wolfensberger TJ, eds. *The Retinal Pigment Epithelium.* New York: Oxford University Press; 1998:103–134.
14. Bialek S, Quong J, Yu K, Miller SS. Nonsteroidal anti-inflammatory drugs alter chloride and fluid transport in bovine retinal pigment epithelium. *Am J Physiol.* 1996;270:C1175–C1189.
15. Edelman JL, Miller SS. Epinephrine stimulates fluid absorption across bovine retinal pigment epithelium. *Invest Ophthalmol Vis Sci.* 1991;32:3033–3040.
16. Hughes BA, Miller SS, Machen TE. Effects of cyclic AMP on fluid absorption and ion transport across frog retinal pigment epithelium: measurements in the open-circuit state. *J Gen Physiol.* 1984;83:875–899.
17. Kita M, Marmor MF. Effects on retinal adhesive force in vivo of metabolically active agents in the subretinal space. *Invest Ophthalmol Vis Sci.* 1992;33:1883–1887.
18. Marmor MF, Maack T. Enhancement of retinal adhesion and subretinal fluid resorption by acetazolamide. *Invest Ophthalmol Vis Sci.* 1982;23:121–124.
19. Marmor MF, Negi A. Pharmacologic modification of subretinal fluid absorption in the rabbit eye. *Arch Ophthalmol.* 1986;104:1674–1677.
20. Peterson W, Meggyesy C, Yu K, Miller SS. Extracellular ATP activates calcium signaling, ion and fluid transport in retinal pigment epithelium. *J Neurosci.* 1997;17:2324–2337.
21. Dougherty RW, Pendergast W, Yerxa BR, et al. INS542 and INS37217: novel P2Y2 receptor agonists with enhanced biological stability induce prolonged stimulation of tracheal mucus velocity *in vivo* (Abstract). *J Aerosol Med.* 1999;12:141.
22. Peterson WM, Venturini AE, Cowlen MS, Vezina M, Piccirilli G. Metabolism, ocular distribution, and ERG effects of INS37217, a novel P2Y2 receptor agonist, for the treatment of retinal detachment [ARVO Abstract]. *Invest Ophthalmol Vis Sci.* 2001;42(4):**S**446. Abstract nr 2408.
23. Joseph DP, Miller SS. Apical and basal membrane ion transport mechanisms in bovine retinal pigment epithelium. *J Physiol (Lond).* 1991;435:439–463.
24. Miller SS, Steinberg RH. Passive ionic properties of frog retinal pigment epithelium. *J Membr Biol.* 1977;36:337–372.
25. Oakley BD, Miller SS, Steinberg RH. Effect of intracellular potassium upon the electrogenic pump of frog retinal pigment epithelium. *J Membr Biol.* 1978;44:281–307.
26. Lin H, Miller SS. Apical epinephrine modulates [Ca2+]i in bovine retinal pigment epithelium [ARVO Abstract]. *Invest Ophthalmol Vis Sci.* 1991;32(4):**S**671. Abstract nr 24.
27. Kenyon E, Maminishkis A, Joseph DP, Miller SS. Apical and basolateral membrane mechanisms that regulated pHi in bovine retinal pigment epithelium. *Am. J. Physiol.* 1997;273:C456–C472.
28. Grynkiewicz G, Poenie M, Tsien RY. A new generation of Ca2+ indicators with greatly improved fluorescence properties. *J Biol Chem.* 1985;260:3440–3450.

29. Daniel WW. *Biostatistics: A Foundation for Analysis in the Heatlh Sciences.* New York: John Wiley & Sons, Inc.; 1995.
30. Mann HB, Whitney DR. On a test of whether one of two random variables is stochastically larger than the other. *Ann Math Stat.* 1947;18:50–60.
31. Peterson WM, Quong JN, Blaug S, Miller SS. Evidence that cyclic-AMP dependent chloride conductance is controlled by phospholamban rather than CFTR in bovine RPE [ARVO Abstract]. *Invest Ophthalmol Vis Sci.* 1997;38(4):**S**467. Abstract nr 2175.
32. Quinn RH, Quong JN, Miller SS. Adrenergic receptor activated ion transport in human fetal retinal pigment epithelium. *Invest Ophthalmol Vis Sci.* 2001;42:255–264.
33. Teixeira M, Ferrary E, Butlen D. UTP binding and phosphoinositidase C activation in ampulla from frog semicircular canal. *Am J Physiol Regul Integr Comp Physiol.* 2000;279:R803–R812.
34. Chan LN, Wang XF, Tsang LL, Chan HC. Pyrimidinoceptors-mediated activation of Ca(2+)-dependent Cl(−) conductance in mouse endometrial epithelial cells. *Biochim Biophys Acta.* 2000;1497:261–270.
35. Gabriel SE, Makhlina M, Martsen E, et al. Permeabilization via the P2X7 purinoreceptor reveals the presence of a Ca2+-activated Cl− conductance in the apical membrane of murine tracheal epithelial cells. *J Biol Chem.* 2000;275:35028–35033.
36. Clarke LL, Harline MC, Gawenis LR, et al. Extracellular UTP stimulates electrogenic bicarbonate secretion across CFTR knockout gallbladder epithelium. *Am J Physiol Gastrointest Liver Physiol.* 2000;279:G132–G138.
37. Miller SS, Edelman JL. Active ion transport pathways in the bovine retinal pigment epithelium. *J Physiol* (*Lond*). 1990;424:283–300.
38. Bialek S, Miller SS. K^+ and Cl^- transport mechanisms in bovine pigment epithelium that could modulate subretinal space volume and composition. *J Physiol* (*Lond*). 1994;475:401–417.
39. Barnard EA, Burnstock G, Webb TE. G protein-coupled receptors for ATP and other nucleotides a new receptor family. *Trends Pharmacol Sci.* 1994;15:67–70.
40. Zimmermann H. Signalling via ATP in the nervous system. *Trends Neurosci.* 1994;17:420–426.
41. Vassort G. Adenosine 5′-triphosphate: a p2-purinergic agonist in the myocardium. *Physiol Rev.* 2001;81:767–806.
42. Taylor CW, Broad LM. Pharmacological analysis of intracellular Ca2+ signalling: problems and pitfalls. *Trends Pharmacol Sci.* 1998;19:370–375.
43. Pozzan T, Rizzuto R, Volpe P, Meldolesi J. Molecular and cellular physiology of intracellular calcium stores. *Physiol Rev.* 1994;74:595–636.
44. Joseph DP, Miller SS. Alpha-1-adrenergic modulation of K and Cl transport in bovine retinal pigment epithelium. *J Gen Physiol.* 1992;99:263–290.
45. Edelman JL, Miller SS. Epinephrine [EP] stimulates KCl and fluid absorption across the bovine retinal pigment epithelium [RPE] [ARVO Abstract]. *Invest Ophthalmol Vis Sci.* 1992;33(4):**S**1111. Abstract nr 2092.
46. Rymer J, Miller SS, Edelman JL. Epinephrine increases intracellular [Ca^{2+}] and stimulates KCl-coupled fluid absorption across bovine retinal pigment epithelium. *Invest Ophthalmol Vis Sci.* 2001;42:1921–1929.
47. Pederson JE. *Fluid Physiology of the Subretinal Space.* In: Wilkinson CP, eds. *Retina.* St. Louis: Mosby; 2001:1870–1881.
48. Lieberman DM. Rationale for abandoning the circumferential wedge resection procedure for high myopia. *J Refract Surg.* 1996;12:635–637.
49. Chihara E, Nao-IN. Transport of subretinal fluid by the retinal pigment epithelium: studies on rhegmatogenous retinal detachment surgery without drainage of the subretinal fluid. *Nippon Ganka Gakkaiz Asshi.* 1984;88:1318–1323.